Front. Phys., 2014, 9(6): 748–759
DOI 10.1007/s11467-014-0424-2

REVIEW ARTICLE

# Conductivity of carbon-based molecular junctions from *ab-initio* methods

**Xiao-Fei Li**[1], **Yi Luo**[2,3,†]

[1] *School of Optoelectronic Information, University of Electronic Science and Technology of China, Chengdu 610054, China*
[2] *Hefei National Laboratory for Physical Sciences at the Microscale, University of Science and Technology of China, Hefei 230026, China*
[3] *KTH, Royal Institute of Technology, School of Biotechnology, Division of Theoretical Chemistry and Biology, S-106 91 Stockholm, Sweden*
*Corresponding author. E-mail:* [†] *luo@kth.se*
*Received March 23, 2014; accepted April 14, 2014*

Carbon nanomaterials (CNMs) are prompting candidates for next generational electronics. In this review we provide a mini overview of recent results on the conductivity of carbon-based molecular junctions obtained from *ab-initio* methods. CNMs used as nanoelectrodes and molecular materials in molecular junctions are discussed. The functionalities that include the nanomechanically controlled molecular conductance switches, negative differential resistance devices, and electronic rectifiers realized by using CNMs have been demonstrated.

**Keywords** carbon nanotubes, graphene, all-carbon nanodevice, quantum transport, *ab-initio* molecular dynamics simulations

**PACS numbers** 31.15.A-, 73.63.-b

Contents



## 1 Introduction

The development of semiconductor industry has totally changed the way people live by continually reducing the size of electronic devices. Now, it is facing the challenge of approaching both physical and material limits [1]. Molecules and nanomaterials are expected to dominate the information technologies in the further, because they are the smallest stable quantum structures with novel functionalities [2, 3].

But the novel properties of them can not always be really used in modern integrated circuits (ICs), due to the simple fact that they first have to be connected to electrodes to form functional devices [4, 5]. In order to extrapolate the intrinsic transport properties of the formed molecular devices [6], nanoelectrodes with a controllable nanogap have to be first fabricated, then the chosen molecule is inserted in the gap with some advanced fabrication technologies [7–16]. The difference of the measured current–voltage ($I$–$V$) characteristics with or without the molecule in the gap reflects the transport properties of the molecule and the formed molecular junctions. Many works in this field [2, 17–21] reveal that the transport properties of molecular junctions are determined not only by the adopted molecule [17, 21], but also the electrode materials [22], and especially the coupling between them [23]. Or to say, the measured properties could not always be the intrinsic properties of the molecules [24–27]. Because many factors can seriously affect the detailed structures of the formed junction, i.e., the adopted electrode materials, the anchoring groups, the roughness of the edges of the formed nanoelectrodes, the multi-active-sites at the edges of electrodes, the configuration of the formed electrode gap, and the configuration of the attached molecules that can be affected by the hydrogen bonds, stacking structures, and so on. Needless to say, the uncontrollable structures can significantly affect the measured properties and hinder the realization

of the desirable functionalities of the molecular devices [7–9, 22, 26, 28–30]. Moreover, organic molecules and metal electrodes have quite different work functions [31], the overlap between the electronic states of molecule and electrode could be very weak. Even if anchoring groups are used, the molecule can still move easily on the surface of metal electrodes, resulting in the unstable structures and uncontrollable conductivity of the formed molecular junctions [28, 32–37].

One possible way to overcome this type of problems is to use carbon materials as both the functional (molecular) material and the nanoelectrode to construct all-carbon molecular devices [39–52]. Due to the all-carbon feature, multi C-C bonds are expected to be formed at the contact region between the molecule and the electrodes (as shown in Fig. 1). Thus the formed devices can have a good stability. It is revealed that the charge mobilities of the polymers [53–55], carbon nanotubes (CNTs) [56–59], and graphene nanoribbons (GNRs) [60, 61] are very high and they are able to withstand a large current density, thus they can be used as functional and electrode materials in molecular devices [44, 61–64].

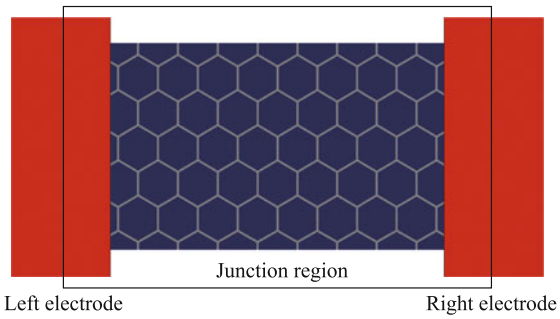


**Fig. 1** A schematic draw of a possible carbon based molecular junction used metal as electrodes [38].

However, the detailed structure of formed contacts and the configuration of the molecular junctions still could be complicated [65–67], and it is very hard to directionally obtain them only by using the physical and chemical intuitions. In some cases, statistical methods like *ab-initio* molecular dynamics (MD) [68] and Monte Carlo (MC) [69] simulations have to be used [70]. Actually, the electron transports are often measured in repeatedly formed junctions and statistical methods are adopted to analyze the large amount of experimental data. Hence, the statistical average is believed to be one of the most meaningful methods for modeling the experimental results. Moreover, environmental factors, including temperature, pressure, solution, small molecule absorption, etc. are very difficult to be treated only using quantum mechanics approaches, but they are relatively convenient to be treated with the combination of quantum mechanics and MD/MC simulations [71].

This review includes our recent results on the multi-scale modeling of the transport properties of carbon-based molecular junctions. Several nanodevices with fascinating structures and attractive properties have been designed by means of state-of-the-art computational methods, which include *ab-initio* MD simulations for the geometry, density functional theory (DFT) [72, 73] for the electronic structure, and non-equilibrium Green's functions (NEGF) [74–79] for carriers transport properties. The using of carbon-based materials as functional molecules, nanoelectrodes and the whole junctions are included.

## 2 Carbon-based functional materials

Carbon allotropes were limited to graphite, diamond, and amorphous carbon until the discovering of $C_{60}$ [80, 81]. Nowadays, new forms of carbon allotropes including fullerenes, carbon nanotubes, and graphene are expected to be the potential basis functional nanomaterials for the next generation of electronic devices.

Carbon nanotubes, as tube-shaped carbon nanomaterials, were first observed in 1991 in the carbon soot of graphite electrodes during an arc discharge [56]. Nowadays, high-quantity CNTs can be well synthesized with various methods [58, 82–89]. It is revealed that the unusual properties of CNTs strongly depend on the combination of their chiral angle and diameter. The single-welled CNTs (SWCNTs) can be represented by a chiral vector $(n, m)$, here the integers $n$ and $m$ denote the number of two unit vectors in the honeycomb crystal lattice of graphene. It is well-known that SWCNTs with $m = 0$ are of zigzag edges, and with $n = m$ are of armchair edges, otherwise they are of chiral edges. When the value $n - m$ is a multiple of 3, the SWCNTs are metallic, in other cases, they are semiconductors with a chiral dependent bandgap [64, 90]. The building of transistors from semiconducting SWCNTs makes it possible to minimize the device dimensions into a few nanometers. Since the experimentally fabricated SWCNTs normally have a diameter of sub-2-nanometer [91], such a individual SWCNT can carry currents with a density exceeding $10^9$ A/cm$^2$ [62], which is about 1000 times larger than that in metals [63].

We have investigated the quantum transport properties of several molecular devices that were constructed by using a short section of CNT as the functional material inserted in the gap between two metal electrodes. When only one CNT is used, the constructed device is denoted as M-CNT-M. When two CNTs are parallelly

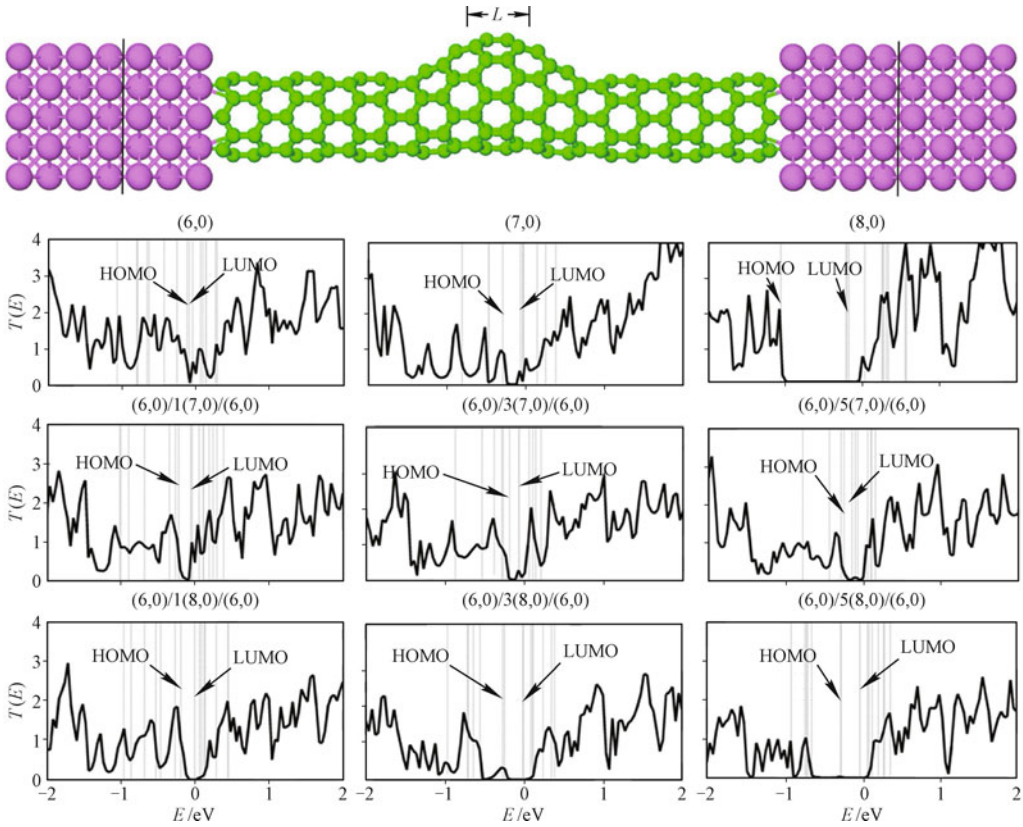


**Fig. 2** The top panel is the optimized structure of device Al-(6,0)/1(8,0)/(6,0)-Al. The bottom panel is the zero-bias transmission spectra of the considered nanodevices. Reproduced from Ref. [92], Copyright © 2007 American Institute of Physics.

placed in the gap the device can be denoted as M-diCNTs-M. If the CNT contains a heterostructure, the device can be denoted as M-heteroCNT-M as shown in Fig. 2.

For practical applications, the typical length of the molecular junction part is less than 10 nm [1]. Pomorski *et al.* proposed that in that short M-CNT-M junctions [43], the evanescent modes were present and their effect on the transport properties cannot be ignored. Our calculations showed that such modes cannot be used for functions in pure M-CNT-M junctions. While, when the CNT contains a heterostructure, the evanescent modes and the electronic transport properties of the devices can be well modulated [92]. Two types of heterostructures (6,0)/$N$(7,0)/(6,0) and (6,0)/$N$(8,0)/(6,0) that are formed by introducing a short section of (7,0) or (8,0) into (6,0) were considered in our calculations. One can see in Fig. 2 that the transmission gap of the system shows a large dependence of the length and the size of the heterojunction due to the semiconducting characteristic of the introduced (7,0) or (8,0) tubes. When the introduced (8,0) tube is long to 5-cells, the conductivity of the highest occupied molecular orbital (HOMO) is totally suppressed and a wide transport gap about 0.75 eV presents in the device (6,0)/5(8,0)/(6,0). More interestingly, negative differential resistance (NDR) behaviors have been observed in the $I$–$V$ characteristics of the devices constructed by certain CNT-heterojunctions, as shown in Fig. 3. One can see in the insert of Fig. 3 that the intensity of the transmission peak near 0.58 eV has been largely reduced with the bias increasing from 1.1 V to 1.2 V and results in the NDR behavior. We attributed this large reduction of transmission to the possibility that the conductivity of the involved evanescent modes are sensitive to the bias applied on those devices.

For M-diCNTs-M devices, we have examined the effect of weak interaction between the bi-tubes on the transport properties of the device [93]. The plots of the frontier molecular orbitals and zero-bias transmissions of the devices were given in Fig. 4. From the figure, one can see that when the intertube distance is large to 3.0 Å, the weak interaction can only induce an energy exchange between the coupled orbitals of the CNTs that can only lead to a small reduction of transmission gap in the system. With the intertube distance reduced, the interaction can be enhanced that can induce the orbital splitting and reduce the transmission gap around Fermi level markedly. When the distance is shorter to 2.3 Å, the conductance gap is reduced to near zero and the system shows obviously metallic behavior.

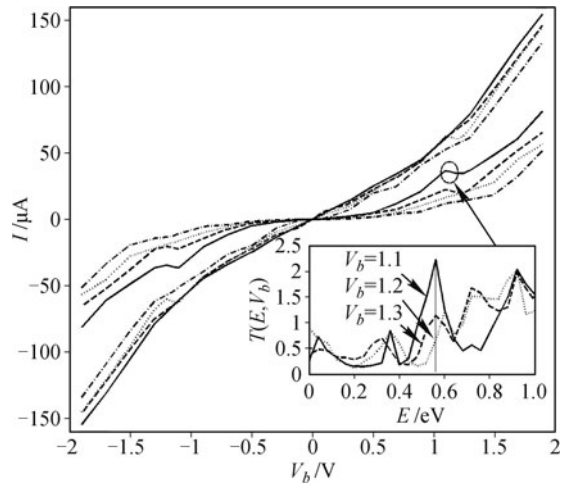


**Fig. 3** The calculated current as the function of the applied bias on CNT-heterojunction devices: The curves are divided into two bundles. The above and below bundles (for positive bias) correspond to (6,0)/$N$(7,0)/(6,0) and (6,0)/$N$(8,0)/(6,0) CNT heterojunctions, respectively. The solid, dashed, dotted, and dot-dashed curves correspond to $N = 1, 2, 3$, and 5, respectively. The insert gives $T(E, V_b)$ of the $(6, 0)/1(8, 0)/(6, 0)$ system under biases $V_b = 1.1$, 1.2, and 1.3 V. Reproduced from Ref. [92], Copyright © 2007 American Institute of Physics.

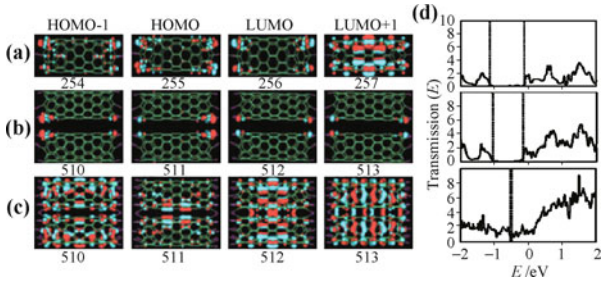


**Fig. 4** The HOMO-1,HOMO, LUMO, LUMO+1 for M-CNT-M device **(a)**, M-diCNTs-M device with a intertube distance of 3.0 Å **(b)** and 2.3 Å **(c)**, and the zero-bias transmission spectra of the three devices **(d)**. Reproduced from Ref. [93], Copyright © 2007 American Institute of Physics.

Above results show that tuning the weak interaction between molecules is one of effective methods to control the transport properties of the electronic devices constructed by multi-CNTs. While introducing heterostructures in CNTs can not only tune the transport properties but also introduce some functionalities into M-CNT-M devices.

## 3 Carbon-based nanoelectrodes

Recently, theoretical and experimental studies have explored the use of CNTs and GNRs as the tips of electrodes for atomic force microscopy (AFM) and scanning tunneling microscope (STM) [94–99] to improve the resolution due to their one-dimensional (1D) nanostructure with very high electrical conductivity and carrier mobility. Especially, it is proposed that they can be used as electrodes in molecular devices [22, 50, 67, 100–102] to excellently enhance the thermal and operational stabilities of the constructed devices [103], because covalent C-C bonds are expected to be formed at the contact region. Moreover, the electronic properties of both CNTs and GNRs can be easily controlled by chirality and doping, which can be used to tune the functionality and the performance of the constructed devices [104–107]. For examples, our first principles results showed that with the proper arrangement of the absorbed oxygen atoms at low concentrations a big bandgap up to 1.58 eV can open in graphene [104], suggesting the potential application of highly reduced graphene oxides in molecular devices. By tuning the location of nitrogen dopant $N_2^{AA}$ in armchair GNRs, the system shows an obvious transition from semiconducting to metallic [105]. Besides the oxygen atom absorption and the nitrogen doping, it is revealed that hydrogenation is also an effectively way to tune the electronic properties of graphene [108–110]. Our first principles calculations showed that the hydrogenated strip can be regarded as a separator to electrically separate a zigzag GNR (ZGNR) into two sub-ZGNRs. Two highly conductive edge-like states can be introduced into the subbands around the Fermi level, which can greatly enhance the conductance of the system [106, 107]. While, with removing the hydrogen atoms at the reconstructed (2,1)-edges of chiral GNRs, a carbene-like structure can be formed at the edges. The introduced edge states make the system change its properties from non-polarization to heavily polarization [111]. Anyway, both CNTs and GNRs could be fascinating electrode materials for nanoelectrodes.

We modeled the mechanical breaking process of the SWCNT for electrodes with *ab-initio* MD simulations [65]. Four snapshots were given in Fig. 5. One can see that the CNT breaks along its chiral angle under the mechanical stretching, the broken areas have pentagon-defects, and the broken ends are quite irregular. The

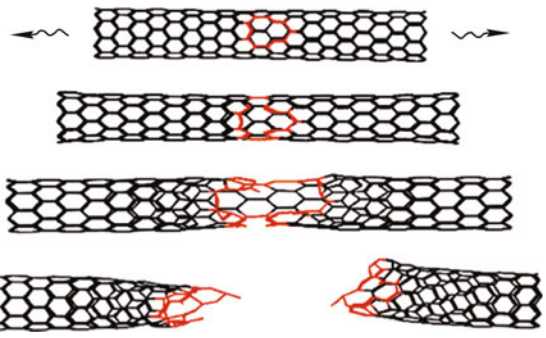

**Fig. 5** Four snapshots of the mechanical breaking process of a (9,0) CNT with a hole defect in the middle of the wall. Reproduced from Ref. [65], Copyright © 2010 American Chemical Society.

edges of the broken ends are mostly of zigzag structure, but the armchair type and dangling bonds of carbon atoms also present randomly. It is noted that the shape of the broken CNT tube obtained from our MD simulations is in good agreement with experimental results [112, 113]. The irregular end is expected to bring in quite rich active sites for molecule attaching that can lead to many different configurations of the obtained CNT-Mol-CNT devices, allowing us to obtain statistically meaningful electron transport properties that could be used to explain several important experimental findings [22, 50].

After obtained the structure of broken CNT-electrodes, we performed *ab-initio* MD simulations to model the reconnecting process of the broken CNT by a single cruciform diamine molecule with two dehydrogenated NHOC- linkers [65]. The determination and controlment of molecular conformation inside a molecular device is one of the most important issues in achieving the reproducible performance. Unfortunately, it seems that using CNTs as electrodes cannot solve this problem. Because our simulation results show that the detailed structures of the broken ends, the nanogap size, and especially the apex of the electrodes are very important factors that dominate the formation of contacts. Since rich active sites are offered for molecule attaching, many contacts and configurations of the molecular bridge in the gap were obtained in our simulations. The chemical structures of the obtained contacts were shown in Fig. 6, and the statistics of the possible contacts and the configurations were listed in Table 1, respectively.

From the Table, we found that the molecule prefers to be titled in the nanogap though either R1-R3 or R2-R2

**Table 1** Statistics of possible contacts between the molecule and the break (9,0) CNT electrode. The detail structures of contacts Z1, Z2, A1, A2, R1, R2, R3, and R4 are shown in Fig. 6. Both parallel (P) or tilted (T) conformations of the molecular bridges are involved. Reproduced from Ref. [65], Copyright © 2010 American Chemical Society.

| Contact | Z1 | | Z2 | | A1 | | A2 | | R1 | | R2 | | R3 | | R4 | | Sum | |
|---|---|---|---|---|---|---|---|---|---|---|---|---|---|---|---|---|---|---|
| | P | T | P | T | P | T | P | T | P | T | P | T | P | T | P | T | P | T |
| Z1 | 0 | 0 | 0 | 0 | 0 | 0 | 0 | 0 | 0 | 0 | 1 | 2 | 2 | 3 | 0 | 1 | 3 | 6 |
| Z2 | 1 | 2 | 1 | 1 | 0 | 1 | 0 | 0 | 1 | 2 | 0 | 0 | 1 | 1 | 1 | 2 | 5 | 9 |
| A1 | 0 | 0 | 0 | 0 | 1 | 0 | 0 | 1 | 0 | 0 | 0 | 2 | 0 | 1 | 0 | 0 | 1 | 4 |
| A2 | 0 | 1 | 0 | 0 | 0 | 0 | 0 | 0 | 0 | 2 | 0 | 0 | 0 | 0 | 1 | 1 | 1 | 4 |
| R1 | 1 | 2 | 0 | 3 | 0 | 0 | 1 | 1 | 0 | 1 | 1 | 3 | 6 | 16 | 1 | 2 | 10 | 28 |
| R2 | 0 | 1 | 0 | 1 | 0 | 0 | 0 | 0 | 0 | 0 | 5 | 10 | 1 | 4 | 0 | 0 | 6 | 16 |
| R3 | 0 | 0 | 0 | 0 | 0 | 0 | 0 | 0 | 0 | 0 | 0 | 0 | 0 | 0 | 0 | 0 | 0 | 0 |
| R4 | 0 | 1 | 0 | 0 | 0 | 0 | 0 | 0 | 0 | 1 | 0 | 1 | 1 | 2 | 0 | 1 | 1 | 6 |
| Sum | 2 | 7 | 1 | 5 | 1 | 1 | 1 | 2 | 1 | 6 | 7 | 18 | 11 | 27 | 3 | 7 | 27 | 73 |

local contacts and to form R(9,0)-R1R3/T or R(9,0)-R2R2/T junctions. Our first principles results showed that the binding energy between the molecule and the CNT for different contacts is of the following order: R1 > R3 > R2 ≫ R4. The transport calculations showed that the conductivity of the formed molecular junction is heavily sensitive to the contacts and the configuration of the molecular bridge. We found that only the statistically and energetically favorable device (R(9,0)-R1R3/T) shows metallic behavior as shown in Fig. 7 due to the highly delocalized HOMO at the Fermi level, that qualitatively agrees with the experimental observation [22, 50]. Other devices we obtained are semiconducting, that disagrees with the experiments. We have also examined the dependence of the chirality of CNTs and found that the edge of the broken CNTs becomes more regular with

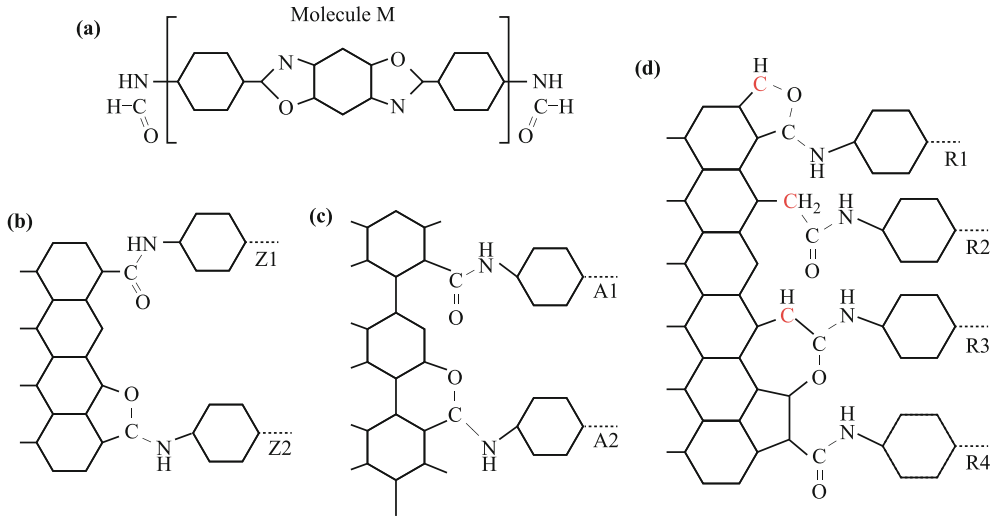


**Fig. 6** **(a)** The chemical structure of a single cruciform diamine molecule (M) with two NHOC-H linkers. Schismatical draws of the contacts between the molecule and **(b)** the zigzag or **(c)** the armchair, or **(d)** the irregular edges of graphene electrodes. Reproduced from Ref. [65], Copyright © 2010 American Chemical Society.

the increase of the chiral angle. This means that the armchair CNTs (with the maximal chiral angle of 30 degree) could be the best choice of electrodes for CNTs-molecular junctions. These findings could be useful for understanding and designing of CNT-based molecular junction or tips of ATM and STM.

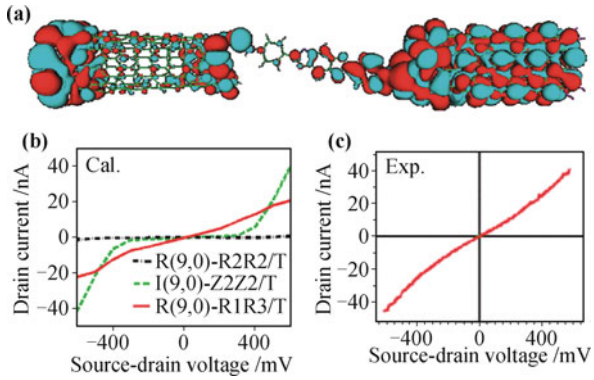


**Fig. 7** **(a)** The molecular projected self-consistent Hamiltonian (MPSH) of the highest occupied molecular orbitals (HOMO) of R(9,0)-R1R3/T junction. **(b)** The calculated current-voltage curves ($I$–$V$) of I(9,0)-Z2Z2/T, R(9,0)-R2R2/T, and R(9,0)-R1R3/T junctions. **(c)** The experimental current-voltage curve of a realistic BCNTs-molecular junction [22]. Reproduced from Ref. [65], Copyright © 2010 American Chemical Society.

Interestingly, our calculations showed that the arrangement of the two electrodes is also an important factor for controlling the transport properties of the obtained molecular junctions [66]. With pushing one of the broken CNT-electrodes down gradually with a step of 0.1 nm (Y-0 to Y-8), the molecular junction changes its configuration from one to another and results in a quite different conductivity as shown in Fig. 8. With this observation, we designed a type of nanomechanically controlled molecular conductance switches and their performances

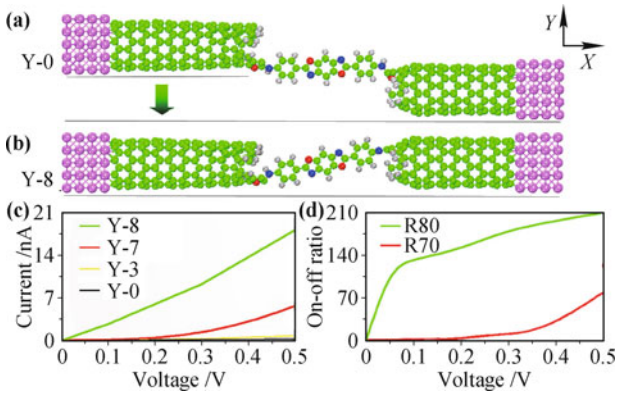


**Fig. 8** **(a)** Structure of BCNT-M junction with low conductance, Y-0; **(b)** Structure of BCNT-M junction with high conductance, Y-8; **(c)** Calculated $I$–$V$ curves for various steps; **(d)** The switch ratio between Y-7 and Y-0 (R70) and between Y-8 and Y-0 (R80). Reproduced from Ref. [66], Copyright © 2009 American Institute of Physics.

have been examined. One can see in the figure that this type of switch can be well switched by moving the electrode only about 0.1 nm. Even at large biases, the switch is still quite stable with a high On/Off ratio up to 200.

One might expect that the graphene could also be good electrode materials. But our calculations showed that rich contacts can be formed between a molecule and GNRs, even when a carbon atomic chain was used as the molecule [52]. Interestingly, a perfect spin filter and a strong current polarization behavior was found in the device when the device has two asymmetrical contacts. This means that understanding the contacts of graphene-graphene, graphene-molecule, graphene-CNT, graphene-metal, graphene-dielectric film, and graphene-semiconductor are of great scientific and technological importance for nanoelectronics [51, 114–116].

## 4 All-carbon junction

Carbon materials have already been used in every aspect of our everyday lives, eg. activated carbons for water purification and carbon black for reinforcing radial tires. All-carbon nanodevices that are expected to be constructed by carbon nanomaterials, eg. fullerenes, CNTs, graphene, and GNRs have attracted enormous interests in nanoelectronics [39, 45–49], due to their extraordinary advantages relative to other devices [39]. Currently, much more attention has been paid on all-carbon heterojunctions, like CNTs-CNTs, CNTs-GNRs, and GNRs-GNRs, due to CNTs and GNRs having 1D structure but quite different electronic properties.

It is well known that the armchair GNRs and zigzag GNRs have very different electronic structure and transport properties. The armchair|zigzag hybrid GNRs (A|Z-hGNRs) are expected to be of interesting properties [117–119]. But theoretically predicting the properties of A|Z-hGNRs remains challenging due to its inhomogeneous structure, which makes supercell model tough to choose. The applicability of supercells with different grain boundaries (GBs) and lattice-mismatches for describing AGNR|ZGNR junction as shown in Fig. 9 was first validated by *ab-initio* MD simulations and first principles electronic structure calculations [120]. Our simulations validated that the supercell containing 4 armchair and 7 zigzag unit cells (4A|7Z) is an appropriate supercell model to describe the system with the minimal strain. One can see in Fig. 9(d) that the choice of different supercell models can result in quite different band structure and spin polarization properties of the system, because of quite different intrinsic strains contained at the GBs regions, which plays a decisive role in determining the

properties of the system. Interestingly, we found that ferromagnetic state is the ground state of the system, which is independent of the choice of the supercell models. But for the case of using the supercell (4A|7Z) with nearly-perfect lattice match, the highest Curie temperature can be achieved, suggesting the potential applications of this material in spin electronics.

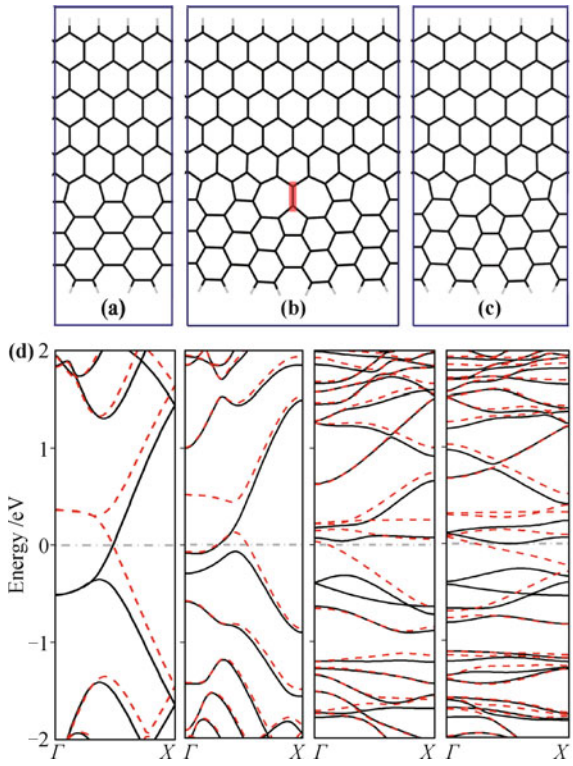


**Fig. 9** Optimized AGNR-ZGNR ribbons that were described with supercell structures 2A|4Z **(a)**, 4A|7Z **(b)**, and 3A|5Z **(c)**, respectively. **(d)** from left to right, it is the calculated band structure of 6-ZGNR, 2A|4Z, 3A|5Z, and 4A|7Z at ferromagnetic state respectively.

After obtaining the appropriate supercell of A|Z-hGNRs, we designed [42] a type of AGNR|ZGNR heterojunctions with different widths as shown in Fig. 10(a). Very interesting transport properties have been found in the systems. One can see in the figure that the A|Z-grain can introduce a size-tunable energy gap in the system. When the width ($N$) of the AGNR fulfills the condition $N = 6p + 5$ (where $p = 1, 2, 3, \cdots$), a sharp transmission peak presents right at the Fermi level, the system has a zero energy gap and shows metallic properties. While if it follows $N = 6p+1$ or $N = 6p+3$, a wide transmission gap appears around the Fermi level and the system shows semiconducting properties. A well-defined zero-bias conductance oscillation with the width increasing presents in the system, which should be originated from the resonance and nonresonance of frontier orbitals between AGNR and ZGNR parts. We also found that the $I$–$V$ characteristics of each junctions possess a pronounced rectifying behavior, and the direction of the rectification oscillates with the increase of the width of the ribbons. A high rectification ratio up to $10^4$ can be achieved with changing the width of the ZGNR to minimize the backward current.

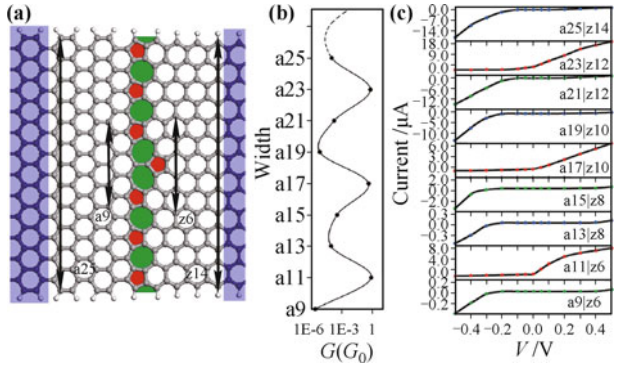


**Fig. 10** **(a)** The fully optimized structure of the AGNR|ZGNR heterojunction labeled as a25|z14, **(b)** zero-bias conductance as a function of the ribbon width, **(c)** the current/voltage characteristics of the AGNR|ZGNR heterojunctions with different widths. Reproduced from Ref. [42], Copyright © 2011 American Chemical Society.

To evaluate the length effect of A/Z-grain, we have also considered another type of AGNR|ZGNR heterojunctions [107] that were constructed by fusing an armchair and a zigzag GNRs side by side. Results showed that the electronic transparency of the junctions is largely dependent on the connection length between the ZGNR and the AGNR. Electronic rectifying behavior is an intrinsic characteristics of the system due to the asymmetrical structure. Our results also suggested that when the asymmetry of the transmission spectra between the holes and electrons can be enhanced with some methods, a high rectifying can be obtained in the system.

The obtained unique rectifying behavior suggests that AGNR|ZGNR heterojunctions would be useful for fabricating molecular rectifiers in the future.

Recently, Wei *et al.* [41] proposed that CNT|GNR junctions can be fabricated by the zinc/acid sputter-etching of SWCNTs. It is well-known that during the etching processes, it is still very hard to control the atomic structure at the contact region. While, the effect of the formed realistic contact on the performance of the CNT/GNR devices has still not been well evaluated, which relates directly to practical applications. We investigated [51] the transport properties of CNT|GNR junctions with different contacts as shown in Fig. 11(a). Our results revealed that although the transmission function is heavy dependent on the shape of contacts, the

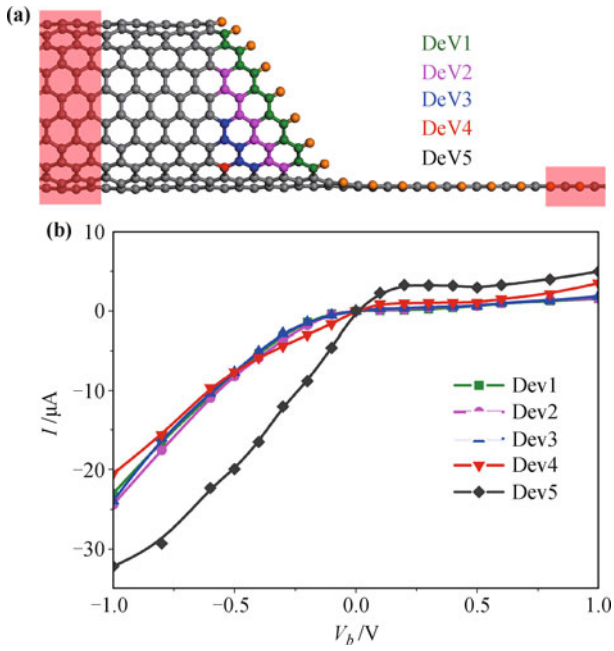


**Fig. 11** **(a)** The geometry of the central scattering region of CNT|GNR, with the edge C atoms at the contact region are marked with different colors for different devices Dev1–5. **(b)** the calculated current as a function of the applied bias for Dev1–5.

rectifying is an inherent property of the system, which is insensitive to the details of contact. In surprise, the realistic contact can enhance the performance of the rectifying and the enhancement is insensitive to the detailed structure of the contact. The stability of the observed rectifying behavior suggests a significant feasibility to manufacture realistic all-carbon rectifiers with CNT|GNR junctions in molecular electronics.

## 5 Conclusions

In conclusion this review article shows the conductivity of carbon-based molecular devices from *ab-initio* calculations. The using of carbon nanomaterials as molecular bridges, electrodes, and the whole molecular junctions are included. Our results showed that *ab-initio* MD simulations can give reasonable description of the realistic ends of the broken CNTs electrodes, the configurations of the fabricated CNT-Mol-CNT junctions, and the detailed structures at the GB region of the AGNR|ZGNR heterojunctions, which is the precondition to design molecular junctions, calculate their electronic structures, examine their transport properties, and compare the obtained results with experimental observations.

We found that the size and length of the CNT-heterojunction plays a significant role in the current-voltage characteristics of nanodevices. NDR behaviors can be observed in the devices constructed with certain heterojunction at certain region [92], and adjusting the weak interaction between two CNTs can significantly change the transport behavior of the junctions [93].

The conductivity of CNT-molecular junction is largely sensitive to the detailed structures of the contacts and the configurations of the molecule in the nanogap. The roughness of the end of the broken CNT-electrodes, especially the apex at the ends, plays an important role in determining the structure of contacts and the configuration of the formed devices [65]. Pushing one of the electrodes to change their arrangements can result in a nanomechanically controlled conductance switch behavior in the devices with a high On/Off ratio [66].

A supercell with a minimal strain and lattice mismatch was obtained, which could be regarded as an appropriate model for describing AGNR|ZGNR heterostructures [120]. With this model, we designed a type of AGNR|ZGNR heterojunction with a well-defined conductance oscillation and striking rectification behavior [42, 107]. It was revealed that the resonance or nonresonance of the frontier orbitals between AGNR and ZGNR is the source of the oscillation and the asymmetric structure is the root of the rectification. A high rectification ratio can be achieved by changing the width of ZGNR to enhance the asymmetric character of transmission function between the holes and electrons, which can minimize the backward current.

The effect of realistic contacts on the performance of the experimentally fabricated CNT|GNR junctions were evaluated [51]. It was found that although the transmission function is heavy dependent on the shape of contacts, the rectifying is an inherent property of the system and its performance can be largely enhance by realistic contacts, suggesting a significant feasibility to manufacture realistic all-carbon rectifiers with CNT|GNR junctions in molecular electronics.

**Acknowledgements** We acknowledge supports by the Major State Basic Research Development Programs (Grant No. 2010CB923300), the National Natural Science Foundation of China (Grant No. 61176116), the Specialized Research Foundation for the Doctoral Program of Higher Education of China (Grant No. 20120161130003), the Swedish Research Council, and the Göran Gustafsson Foundation for Research in Natural Sciences and Medicine. The simulations were performed on resources provided by the Swedish National Infrastructure for Computing (SNIC) at PDC and NSC.

## References and notes

1. The International Technology Roadmap for Semiconductors, 2011. Available at http://www.itrs.net. Accessed July 2012
2. H. Choi and C. C. M. Mody, The long history of molecular electronics: Microelectronics origins of nanotechnology, *Soc.*

*Stud. Sci.*, 2009, 39(1): 11

3. R. S. Mulliken, Structures of complexes formed by halogen molecules with aromatic and with oxygenated solvents, *J. Am. Chem. Soc.*, 1950, 72(1): 600
4. N. B. Zhitenev, A. Erbe, Z. Bao, W. Jiang, and E. Garfunkel, Molecular nano-junctions formed with different metallic electrodes, *Nanotechnology*, 2005, 16(4): 495
5. N. S. Hush, An overview of the first half-century of molecular electronics, *Ann. N. Y. Acad. Sci.*, 2003, 1006(1): 1
6. T. Li, W. Hu, and D. Zhu, Nanogap electrodes, *Adv. Mater.*, 2010, 22(2): 286
7. J. J. Parks, A. R. Champagne, G. R. Hutchison, S. Flores-Torres, H. D. Abruña, and D. C. Ralph, Tuning the Kondo effect with a mechanically controllable break junction, *Phys. Rev. Lett.*, 2007, 99: 026601
8. B. Xu and N. Tao, Measurement of single-molecule resistance by repeated formation of molecular junctions, *Science*, 2003, 301(5637): 1221
9. J. Chen, M. A. Reed, A. M. Rawlett, and J. M. Tour, Large on-off ratios and negative differential resistance in a molecular electronic device, *Science*,1999, 286(5444): 1550
10. J. Park, A. N. Pasupathy, J. I. Goldsmith, C. Chang, Y. Yaish, J. R. Petta, M. Rinkoski, J. P. Sethna, H. D. Abruña, P. L. McEuen, and D. C. Ralph, Coulomb blockade and the Kondo effect in single-atom transistors, *Nature*, 2002, 417: 722
11. C. Z. Li, A. Bogozi, W. Huang, and N. J. Tao, Fabrication of stable metallic nanowires with quantized conductance, *Nanotechnology*, 1999, 10(2): 221
12. J. O. Lee, G. Lientschnig, F. Wiertz, M. Struijk, R A J. Janssen, R. Egberink, D. N. Reinhoudt, P. Hadley, and C. Dekker, Absence of strong gate effects in electrical measurements on phenylene-based conjugated molecules, *Nano Lett.*, 2003, 3(2): 113
13. S. Kubatkin, A. Danilov, M. Hjort, J. Cornil, J.-L. Brédas, N. Stuhr-Hansen, P. Hedegård, and T. Bjørnholm, Single-electron transistor of a single organic molecule with access to several redox states, *Nature*, 2003, 425: 698
14. L. Qin, S. Park, L. Huang, and C. Mirkin, On-wire lithography, *Science*, 2005, 309(5731): 113
15. A. Hatzor and P. S. Weiss, Molecular rulers for scaling down nanostructures, *Science*, 2001, 291(5506): 1019
16. R. Krahne, A. Yacoby, H. Shtrikman, I. Bar-Joseph, T. Dadosh, and J. Sperling, Fabrication of nanoscale gaps in integrated circuits, *Appl. Phys. Lett.*, 2002, 81(4): 730
17. A. Aviram and M. A. Ratner, Molecular rectifiers, *Chem. Phys. Lett.*, 1974, 29(2): 277
18. C. J. Cattena, R. A. Bustos-Marun, and H. M. Pastawski, Crucial role of decoherence for electronic transport in molecular wires: Polyaniline as a case study, *Phys. Rev. B*, 2010, 82(14): 144201
19. B. L. Feringa, R. A. van Delden, N. Koumura, and E. M. Geertsema, Chiroptical molecular switches, *Chem. Rev.*, 2000, 100(5): 1789
20. S. Kubatkin, A. Danilov, M. Hjort, J. Cornil, J.-L. Brédas, N. Stuhr-Hansen, P. Hedegård, and T. Bjørnholm, Single-electron transistor of a single organic molecule with access to several redox states, *Nature*, 2003, 425: 698
21. J. Chen, M. A. Reed, A. M. Rawlett, and J. M. Tour, Large on-off ratios and negative differential resistance in a molecular electronic device, *Science*, 1999, 286(5444): 1550
22. X. Guo, J. P. Small, J. E. Klare, Y. Wang, M. S. Purewal, I. W. Tam, B. H. Hong, R. Caldwell, L. Huang, S. O'Brien, J. Yan, R. Breslow, S. J. Wind, J. Hone, P. Kim, and C. Nuckolls, Covalently bridging gaps in single-walled carbon nanotubes with conducting molecules, *Science*, 2006, 311(5759): 356
23. S. Chung, J. B. Parker, M. Bianchet, L. M. Amzel, and J. T. Stivers, Impact of linker strain and flexibility in the design of a fragment-based inhibitor, *Nat. Chem. Biol.*, 2009, 5(6): 407
24. R. McCreery and A. Bergren, Progress with molecular electronic junctions: Meeting experimental challenges in design and fabrication, *Adv. Mater.*, 2009, 21(43): 4303
25. G. J. Iafrate and M. A. Stroscio, Application of quantum-based devices: Trends and challenges, *IEEE Trans. Electron. Dev.*, 1996, 43(10): 1621
26. X. F. Li, H. Ren, L. L. Wang, K. Q. Cheng, J. Yang, and Y. Luo, Important structural factors controlling the conductance of DNA pairs in molecular junctions, *J. Phys. Chem. C*, 2010, 114(33): 14240
27. M. Q. Long, L. Wang, K. Q. Chen, X. F. Li, B. Zou, and Z. Shuai, Coupling effect on the electronic transport through dimolecular junctions, *Phys. Lett. A*, 2007, 365(5–6): 489
28. J. Heath, Molecular electronics, *Annu. Rev. Mater. Res.*, 2009, 39(1): 1
29. Y. B. Hu, Y. Zhu, H. J. Gao, and H. Guo, Conductance of an ensemble of molecular wires: A statistical analysis, *Phys. Rev. Lett.*, 2005, 95(15): 156803
30. Z. Liu, S. Y. Ding, Z. B. Chen, X. Wang, J. H. Tian, J. R. Anema, X. S. Zhou, D. Y. Wu, B. W. Mao, X. Xu, B. Ren, and Z. Q. Tian, Revealing the molecular structure of single-molecule junctions in different conductance states by fishing-mode tip-enhanced Raman spectroscopy, *Nat. Commun.*, 2011, 2: 305
31. N. B. Zhitenev, W. Jiang, A. Erbe, Z. Bao, E. Garfunkel, D. M. Tennant, and R. A. Cirelli, Control of topography, stress and diffusion at molecule–metal interfaces, *Nanotechnology*, 2006, 17(5): 1272
32. J. M. Seminario, C. E. De La Cruz, and P. A. Derosa, A theoretical analysis of metal–molecule contacts, *J. Am. Chem. Soc.*, 2001, 123(23): 5616
33. J. Kushmerick, D. Holt, J. Yang, J. Naciri, M. Moore, and R. Shashidhar, Metal-molecule contacts and charge transport across monomolecular layers: Measurement and theory, *Phys. Rev. Lett.*, 2002, 89(8): 086802
34. A. Bonifas, and R. McCreery, 'Soft' Au, Pt and Cu contacts

for molecular junctions through surface-diffusion-mediated deposition, *Nat. Nanotechnol.*, 2010, 5(8): 612

35. C.-H. Ko, M.-J. Huang, M.-D. Fu, and C.-H. Chen, Superior contact for single-molecule conductance: Electronic coupling of thiolate and isothiocyanate on Pt, Pd, and Au, *J. Am. Chem. Soc.*, 2009, 132: 756
36. A. K. Patra, S. Singh, B. Barin, Y. Lee, J.-H. Ahn, E. del Barco,E. R. Mucciolo, and B. Özyilmaz, Dynamic spin injection into chemical vapor deposited grapheme, *Appl. Phys. Lett.*, 2012, 101(16): 162407
37. J. Beebe, B. Kim, C. Frisbie, and J. Kushmerick, Measuring relative barrier heights in molecular electronic junctions with transition voltage spectroscopy, *ACS Nano*, 2008, 2(5): 827
38. X. F. Li, *Electron and Spin Transport in Graphene-Based Nanodevices*, Ph.D. thesis, KTH, Theoretical Chemistry and Biology, 2013
39. B. Li, X. Cao, H. G. Ong, J. W. Cheah, X. Zhou, Z. Yin, H. Li, J. Wang, F. Boey, W. Huang, and H. Zhang, All-carbon electronic devices fabricated by directly grown single-walled carbon nanotubes on reduced graphene oxide electrodes, *Adv. Mater.*, 2010, 22(28): 3058
40. P. Avouris, Z. Chen, and V. Perebeinos, Carbon-based electronics, *Nat. Nanotechnol.*, 2007, 2(10): 605
41. D. Wei, L. Xie, K. K. Lee, Z. Hu, S. Tan, W. Chen, C. H. Sow, K. Chen, Y. Liu, and A. T. S. Wee, Controllable unzipping for intramolecular junctions of graphene nanoribbons and single-walled carbon nanotubes, *Nat. Commun.*, 2013, 4: 1374
42. X. F. Li, L. L. Wang, K. Q. Chen, and Y. Luo, Design of graphene-nanoribbon heterojunctions from first principles, *J. Phys. Chem. C*, 2011, 115(25): 12616
43. P. Pomorski, C. Roland, and H. Guo, Quantum transport through short semiconducting nanotubes: A complex band structure analysis, *Phys. Rev. B*, 2004, 70(11): 115408
44. S. Frank, P. Poncharal, Z. L. Wang, and W. A. de Heer, Carbon nanotube quantum resistors, *Science*, 1998, 280(5370): 1744
45. B. Wei, R. Spolenak, P. Kohler-Redlich, M. Ruhle, and E. Arzt, Electrical transport in pure and boron-doped carbon nanotubes, *Appl. Phys. Lett.*, 1999, 74(21): 3149
46. V. Strong, S. Dubin, M. F. El-Kady, A. Lech, Y. Wang, B. H. Weiller, and R. B. Kaner, Patterning and electronic tuning of laser scribed graphene for flexible all-carbon devices, *ACS Nano*, 2012, 6(2): 1395
47. L. Chico, V. H. Crespi, L. X. Benedict, S. G. Louie, and M. L. Cohen, Pure carbon nanoscale devices: Nanotube heterojunctions, *Phys. Rev. Lett.*, 1996, 76(6): 971
48. Z. Yao, H. W. C. Postma, L. Balents, and C. Dekker, Carbon nanotube intramolecular junctions, *Nature*, 1999, 402(6759): 273
49. W. Lu, G. Ruan, B. Genorio, Y. Zhu, B. Novosel, Z. Peng, and J. M. Tour, Functionalized graphene nanoribbons *via* anionic polymerization initiated by Alkali metal-intercalated carbon nanotubes, *ACS Nano*, 2013, 7(3): 2669
50. X. Guo, A. Gorodetsky, J. Hone, J. Barton, and C. Nuckolls, Conductivity of a single DNA duplex bridging a carbon nanotube gap, *Nat. Nanotechnol.*, 2008, 3(3): 163
51. X. H. Zhang, X. F. Li, L. L. Wang, L. Xu, and K. W. Luo, Realistic-contact-induced enhancement of rectifying in carbon-nanotube/graphene-nanoribbon junctions, *Appl. Phys. Lett.*, 2014, 104(10): 103107
52. T. Chen, X. F. Li, L. Wang, K. Luo, Q. Li, X. Zhang, and X. Shang, Perfect spin filter and strong current polarization in carbon atomic chain with asymmetrical connecting points, *Europhys. Lett.*, 2014, 105(5): 57003
53. A. Heeger, Semiconducting and metallic polymers: The fourth generation of polymeric materials (Nobel lecture), *Angew. Chem. Int. Ed.*, 2001, 40(14): 2591
54. Y. Liang, Y. Wu, D. Feng, S. Tsai, H. Son, G. Li, and L. Yu, Development of new semiconducting polymers for high performance solar cells, *J. Am. Chem. Soc.*, 2009, 131(1): 56
55. C. Cattena, R. Bustos-Marún, and H. Pastawski, Crucial role of decoherence for electronic transport in molecular wires: Polyaniline as a case study, *Phys. Rev. B*, 2010, 82(14): 144201
56. S. Iijima, Helical microtubules of graphitic carbon, *Nature*, 1991, 354(6348): 56
57. T. Ebbesen and P. Ajayan, Large-scale synthesis of carbon nanotubes, *Nature*, 1992, 358(6383): 220
58. G. Zhong, J. H. Warner, M. Fouquet, A. W. Robertson, B. Chen, and J. Robertson, Growth of ultrahigh density single-walled carbon nanotube forests by improved catalyst design, *ACS Nano*, 2012, 6(4): 2893
59. X. Wang, Q. Li, J. Xie, Z. Jin, J. Wang, Y. Li, K. Jiang, and S. Fan, Fabrication of ultralong and electrically uniform single-walled carbon nanotubes on clean substrates, *Nano Lett.*, 2009, 9(9): 3137
60. K. Novoselov, A. Geim, S. Morozov, D. Jiang, Y. Zhang, S. Dubonos, I. Grigorieva, and A. Firsov, Electric field effect in atomically thin carbon films, *Science*, 2004, 306(5696): 666
61. A. Geim and K. Novoselov, The rise of graphene, *Nat. Mater.*, 2007, 6(3): 183
62. Z. Yao, C. L. Kane, and C. Dekker, High-field electrical transport in single-wall carbon nanotubes, *Phys. Rev. Lett.*, 2000, 84(13): 2941
63. S. Hong and S. Myung, Nanotube Electronics: A flexible approach to mobility, *Nat. Nanotechnol.*, 2007, 2(4): 207
64. J. C. Charlier, X. Blase, and S. Roche, Electronic and transport properties of nanotubes, *Rev. Mod. Phys.*, 2007, 79(2): 677
65. X. F. Li, K. Q. Chen, L. Wang, and Y. Luo, Effects of interface roughness on electronic transport properties of nanotube molecule nanotube junctions, *J. Phys. Chem. C*, 2010, 114(28): 12335

66. X. F. Li, L. Wang, K. Q. Chen, and Y. Luo, Nanomechanically induced molecular conductance switch, *Appl. Phys. Lett.*, 2009, 95(23): 232118

67. C. Thiele, H. Vieker, A. Beyer, B. S. Flavel, F. Hennrich, D. Munoz Torres, T. R. Eaton, M. Mayor, M. M. Kappes, A. Golzhauser, H. Löhneysen, and R. Krupke, Fabrication of carbon nanotube nanogap electrodes by helium ion sputtering for molecular contacts, *Appl. Phys. Lett.*, 2014, 104(10): 103102

68. B. J. Alder and T. E. Wainwright, Studies in molecular dynamics (I): General method, *J. Chem. Phys.*, 1959, 31(2): 459

69. W. M. C. Foulkes, L. Mitas, R. J. Needs, and G. Rajagopal, Quantum Monte Carlo simulations of solids, *Rev. Mod. Phys.*, 2001, 73(1): 33

70. A. Szabo and N. S. Ostlund, *Modern Quantum Chemistry: Introduction to Advanced Electronic Structure Theory*, New York: MacMillan, 1982

71. W. R. French, C. R. Iacovella, and P. T. Cummings, Large-scale atomistic simulations of environmental effects on the formation and properties of molecular junctions, *ACS Nano*, 2012, 6(3): 2779

72. R. M. Dreizler and E. K. U. Gross, *Density Functional Theory*, Berlin: Springer, 1990

73. W. Koch and M. C. Holthausen, *A Chemistry's Guide to Density Functional Theory*, Verlag: Wiley-VCH, 2001

74. H. Haug and A. P. Jauho, *Quantum Kinetics in Transport and Optics of Semi-conductors*, New York: Springer-Verlag, 1998

75. J. Taylor, H. Guo, and J. Wang, Ab initio modeling of quantum transport properties of molecular electronic devices, *Phys. Rev. B*, 2001, 63(24): 245407

76. M. Brandbyge, J. L. Mozos, P. Ordej'on, J. Taylor, and K. Stokbro, Density-functional method for nonequilibrium electron transport, *Phys. Rev. B*, 2002, 65(16): 165401

77. Y. Xue, S. Datta, and M. A. Ratner, First-principles based matrix Green's function approach to molecular electronic devices: general formalism, *Chem. Phys.*, 2002, 281(2–3): 151

78. J. E. Subotnik, T. Hansen, M. A. Ratner, and A. Nitzan, Nonequilibrium steady state transport via the reduced density matrix operator, *J. Chem. Phys.*, 2009, 130(14): 144105

79. S. Yeganeh, M. A. Ratner, M. Galperin, and A. Nitzan, Transport in state space: Voltage-dependent conductance calculations of benzene-1,4-dithiol, *Nano Lett.*, 2009, 9(5): 1770

80. H. Pierson, *Handbook of carbon, graphite, diamond and fullerenes*, Noyes publications, 1993

81. H. W. Kroto, J. R. Heath, S. C. O'Brien, R. F. Curl, and R. E. Smalley, $C_{60}$: Buckminsterfullerene, *Nature*, 1985, 318(6042): 162

82. P. Collins and P. Avouris, Nanotubes for electronics, *Sci. Am.*, 2000, 283(6): 62

83. T. Guo, P. Nikolaev, A. Rinzler, D. Tomanek, D. Colbert, and R. Smalley, Self-assembly of tubular fullerenes, *J. Phys. Chem.*, 1995, 99(27): 10694

84. T. Guo, P. Nikolaev, A. Thess, D. Colbert, and R. Smalley, Catalytic growth of single-walled manotubes by laser vaporization, *Chem. Phys. Lett.*, 1995, 243(1–2): 49

85. N. Inami, M. Ambri Mohamed, E. Shikoh, and A. Fujiwara, Synthesis-condition dependence of carbon nanotube growth by alcohol catalytic chemical vapor deposition method, *Sci. Technol. Adv. Mater.*, 2007, 8(4): 292

86. N. Ishigami, H. Ago, K. Imamoto, M. Tsuji, K. Iakoubovskii, and N. Minami, Crystal plane dependent growth of aligned single-walled carbon nanotubes on sapphire, *J. Am. Chem. Soc.*, 2008, 130(30): 9918

87. S. Sen and I. Puri, Flame synthesis of carbon nanofibres and nanofibre composites containing encapsulated metal particles, *Nanotechnology*, 2004, 15(3): 264

88. T. Tanaka, H. Jin, Y. Miyata, S. Fujii, H. Suga, Y. Naitoh, T. Minari, T. Miyadera, K. Tsukagoshi, and H. Kataura, Simple and scalable gel-based separation of metallic and semiconducting carbon nanotubes, *Nano Lett.*, 2009, 9(4): 1497

89. H. Liu, D. Nishide, T. Tanaka, and H. Kataura, Large-scale single-chirality separation of single-wall carbon nanotubes by simple gel chromatography, *Nat. Commun.*, 2011, 2: 309

90. X. Lu and Z. Chen, Curved Pi-conjugation, aromaticity, and the related chemistry of small fullerenes ($<C_{60}$) and single-walled carbon nanotubes, *Chem. Rev.*, 2005, 105(10): 3643

91. J. K. Holt, H. G. Park, Y. Wang, M. Stadermann, A. B. Artyukhin, C. P. Grigoropoulos, A. Noy, and O. Bakajin, Fast mass transport through sub-2-nanometer carbon nanotubes, *Science*, 2006, 312(5776): 1034

92. X. F. Li, K. Q. Chen, L. Wang, M. Q. Long, B. S. Zou, and Z. Shuai, Effect of length and size of heterojunction on the transport properties of carbon-nanotube devices, *Appl. Phys. Lett.*, 2007, 91(13): 133511

93. X. F. Li, K. Q. Chen, L. L. Wang, M. Q. Long, B. S. Zou, and Z. Shuai, Effect of intertube interaction on the transport properties of a carbon double-nanotube device, *J. Appl. Phys.*, 2007, 101(6): 064514

94. N. R. Wilson and J. V. Macpherson, Carbon nanotube tips for atomic force microscopy, *Nat. Nanotechnol.*, 2009, 4(8): 483

95. J. Liu, J. K. Notbohm, R. W. Carpick, and K. T. Turner, Method for characterizing nanoscale wear of atomic force microscope tips, *ACS Nano*, 2010, 4(7): 3763

96. K. Meinander, T. N. Jensen, S. B. Simonsen, S. Helveg, and J. V. Lauritsen, Quantification of tip-broadening in non-contact atomic force microscopy with carbon nanotube tips, *Nanotechnology*, 2012, 23(40): 405705

97. J. V. Macpherson, Scanning probe microscopy: Taking a closer look at conductivity, *Nat. Nanotechnol.*, 2011, 6(2): 84

98. Y. Lisunova, I. Levkivskyi, and P. Paruch, Ultrahigh currents in dielectric-coated carbon nanotube probes, *Nano Lett.*, 2013, 13(9): 4527

99. C. Kranz, Recent advancements in nanoelectrodes and nanopipettes used in combined scanning electrochemical microscopy techniques, *Analyst*, 2013, 139(2): 336

100. F. Xiong, A. D. Liao, D. Estrada, and E. Pop, Low-power switching of phase-change materials with carbon nanotube electrodes, *Science*, 2011, 332(6029): 568

101. K. Gong, S. Chakrabarti, and L. Dai, Electrochemistry at carbon nanotube electrodes: Is the nanotube tip more active than the sidewall? *Angew. Chem. Int. Ed.*, 2008, 47(29): 5446

102. M. Del Valle, R. Guti'errez, C. Tejedor, and G. Cuniberti, Tuning the conductance of a molecular switch, *Nat. Nanotechnol.*, 2007, 2(3): 176

103. G. Wang, Y. Kim, M. Choe, T. W. Kim, and T. Lee, A new approach for molecular electronic junctions with a multilayer graphene electrode, *Adv. Mater.*, 2011, 23(6): 755

104. K. Y. Lian, Y. F. Ji, X. F. Li, M. X. Jin, D. J. Ding, and Y. Luo, Big bandgap in highly reduced graphene oxides, *J. Phys. Chem. C*, 2013, 117: 6049

105. T. Chen, X. F. Li, L. L. Wang, Q. Li, K. W. Luo, X. H. Zhang, and L. Xu, Semiconductor to metal transition by tuning the location of N2AA in armchair graphene nanoribbons, *J. Appl. Phys.*, 2014, 115(5): 053707

106. X. F. Li, L. L. Wang, K. Q. Chen, and Y. Luo, Tuning the electronic transport properties of zigzag graphene nanoribbons via hydrogenation separators, *J. Phys. Chem. C*, 2011, 115(49): 24366

107. X. F. Li, L. L. Wang, K. Q. Chen, and Y. Luo, Electronic transport through zigzag/armchair graphene nanoribbon heterojunctions, *J. Phys.: Condens. Matter*, 2012, 24(9): 095801

108. R. Balog, B. Jorgensen, L. Nilsson, M. Andersen, E. Rienks, M. Bianchi, M. Fanetti, E. Laegsgaard, A. Baraldi, S. Lizzit, Z. Sljivancanin, F. Besenbacher, B. Hammer, T. G. Pedersen, P. Hofmann, and L. Hornekaer, Bandgap opening in graphene induced by patterned hydrogen adsorption, *Nat. Mater.*, 2010, 9(4): 315

109. H. J. Xiang, E. J. Kan, S. H. Wei, X. G. Gong, and M. H. Whangbo, Thermodynamically stable single-side hydrogenated graphene, *Phys. Rev. B*, 2010, 82(16): 165425

110. H. L. Gao, L. Wang, J. J. Zhao, F. Ding, and J. P. Lu, Band gap tuning of hydrogenated graphene: H coverage and configuration dependence, *J. Phys. Chem. C*, 2011, 115(8): 3236

111. X. F. Li, L. L. Wang, K. Q. Chen, and Y. Luo, Strong current polarization and negative differential resistance in chiral graphene nanoribbons with reconstructed (2,1)-edges, *Appl. Phys. Lett.*, 2012, 101(7): 073101

112. Y. Wei, K. Jiang, L. Liu, Z. Chen, and S. Fan, Vacuum-breakdown-induced needle-shaped ends of multiwalled carbon nanotube yarns and their field emission applications, *Nano Lett.*, 2007, 7(12): 3792

113. J. Huang, S. Chen, Z. Ren, Z. Wang, K. Kempa, M. Naughton, G. Chen, and M. Dresselhaus, Enhanced ductile behavior of tensile-elongated individual double-walled and triple-walled carbon nanotubes at high temperatures, *Phys. Rev. Lett.*, 2007, 98(18): 185501

114. S. Barraza-Lopez, M. Vanevi'c, M. Kindermann, and M. Y. Chou, Effects of metallic contacts on electron transport through graphene, *Phys. Rev. Lett.*, 2010, 104(7): 076807

115. R. Addou, A. Dahal, and M. Batzill, Growth of a two-dimensional dielectric monolayer on quasi-freestanding graphene, *Nat. Nanotechnol.*, 2012, 8(1): 41

116. F. Xia, V. Perebeinos, Y. M. Lin, Y. Q. Wu, and P. Avouris, The origins and limits of metal–grapheme junction resistance, *Nat. Nanotechnol.*, 2011, 6: 179

117. O. Yazyev and S. Louie, Electronic transport in polycrystalline graphene, *Nat. Mater.*, 2010, 9(10): 806

118. J. Zhou, T. Hu, J. Dong, and Y. Kawazoe, Ferromagnetism in a graphene nanoribbon with grain boundary defects, *Phys. Rev. B*, 2012, 86(3): 035434

119. A. R. Botello-Méndez, E. Cruz-Silva, F. Lopez-Urias, B. G. Sumpter, V. Meunier, M. Terrones, and H. Terrones, Spin polarized conductance in Hybrid graphene nanoribbons using 57 defects, *ACS Nano*, 2009, 3(11): 3606

120. K. Y. Lian, X. F. Li, S. Duan, M. X. Jin, D. J. Ding, and Y. Luo, Tuning electronic and magnetic properties of armchair|zigzag hybrid graphene nanoribbons by the choice of supercell model of grain boundaries, *J. Appl. Phys.*, 2014, 115(10): 104303